

DISTRIBUTION OF WAVE CRESTS IN NON-GAUSSIAN SEA

Ronald W. Butler¹, Ulla B. Machado^{2,3}, Igor Rychlik^{4,5}

¹ Department of Statistics, Colorado State University,
Fort Collins, USA

² Department of Mathematical Statistics, Chalmers University of Technology,
Gothenburg, Sweden

³ Fraunhofer-Chalmers Research Centre for Industrial Mathematics,
Gothenburg, Sweden

⁴ Centre for Mathematical Sciences, Lund University,
Lund, Sweden

ABSTRACT

The sea elevation at a fixed point is modelled as a quadratic form of a vector valued Gaussian process with arbitrary mean. An apparent wave is a part of the sea record observed between two successive upcrossings of the still water level. Saddlepoint methods are used to approximate the mean upcrossing intensity $\mu^+(\mathbf{u})$, say, with which the sea level crosses upwards at height \mathbf{u} . This estimated intensity is further used to determine the density of crest height. Several numerical examples are given.

KEY WORDS: Crest distribution, non-Gaussian sea, Rice's formula, Saddlepoint method.

INTRODUCTION AND MOTIVATION

Commonly the sea surface elevation at a fixed point is modelled as a Gaussian process which, during a limited period of time (1-3 hours), can be considered stationary. The model is called Gaussian sea, and the parameters that characterize its power spectrum are the *sea state*. In reliability analysis of ocean structures the distribution of crest height, denoted by A_c , is often required. The exact form of the distribution is not known. For a Gaussian sea it is a common practice to approximate the A_c -distribution by means of the Rayleigh distribution, given on the right hand side of Eq. 3. The approximation is very accurate for high crests or for seas with narrow band spectrum. However, it is a well known fact that for steep waves in deep waters, or as the water depths decreases, the sea surface profile departs from the Gaussian assumption. Under these conditions the wave profile becomes asymmetric, with higher and steeper crests, and shallower and flatter

troughs. The Gaussian sea model can lead to circa 20% under estimation of wave crests. In this case an application of Rayleigh distribution becomes nonconservative and hence the asymmetry of the sea waves should not be neglected in the reliability analysis of ocean structures.

In this paper we shall present a new method to approximate the distribution of wave crest heights for the non-Gaussian model of the sea elevation. Our approach is based on the following result shown in Rychlik (1993), see also Rychlik and Leadbetter (2000),

$$P(A_c > h) \leq \frac{\mu^+(h)}{\mu^+(m)}, \quad (1)$$

where $\mu^+(h)$ is the intensity which the sea elevation crosses level h in an upward direction and m is the so-called *still water level*, often taken to be the mean value of the sea elevation or the most frequently crossed level, which coincides for the Gaussian sea.

For the Gaussian sea, with still water level $m = 0$, the upcrossing intensity $\mu^+(h)$, is given by the celebrated Rice's formula, (Rice, 1944,1945),

$$\mu^+(h) = \frac{1}{T_z} e^{-8\left(\frac{h}{H_s}\right)^2}, \quad (2)$$

where T_z is the average wave period, and H_s is the significant wave height which is equal to four times the standard deviation of the process. (Note that T_z, H_s are often identified with the sea state.) It is now easy to see that the Rayleigh approximation is conservative in the sense that

$$P(A_c > h) \leq e^{-8\left(\frac{h}{H_s}\right)^2}. \quad (3)$$

Since the Rayleigh approximation is the most commonly used method to derive the crest height distribution for Gaussian sea models, we propose to use Eq. 1 to extend the approximation to non-Gaussian seas. In order to derive the approximation,

⁵Research supported in part by the Gothenburg Stochastic Centre

we first need to specify the probabilistic properties of the non-Gaussian sea and then to compute the crossing intensity $\mu^+(h)$. In this paper we use a quadratic model for the sea surface elevation which takes into account second-order non-linearities (Hasselmann, 1962). The model will be shortly described in the following subsection. Unfortunately there is no explicit formula for the crossing intensity $\mu^+(u)$ for this model. There exists a very accurate numerical method (computation of a three dimensional complex integral) that gives very accurate numerical values for $\mu^+(u)$; see Næss and Machado (2000). However the method is slow, difficult to automate and can be unstable for high levels h . Consequently, in the third section, we present a new method to estimate $\mu^+(u)$, which is not as accurate as the method used by Næss and Machado (2000), but very fast and numerically stable. Finally in the last section we present several examples which consider the accuracy of the new approach for narrow-band Stokes waves, and a quadratic model for the sea elevation in deep and shallow waters. The accuracy is quite good in all the examples.

MODELLING OF THE SEA SURFACE

We begin with the linear sea model, which postulates that the sea surface is a sum of simple cosine waves. In this paper we consider only long crested sea, i.e. the surface does not depend on the y coordinate. In addition we consider an unidirectional sea, where all waves travel along the x axis with positive velocity. The linear sea η_l , consisting of N cosine waves, is given by

$$\eta_l(x, t) = \sum_{n=-N}^N \frac{A_n}{2} e^{i(\omega_n t - \kappa_n x)}, \quad (4)$$

where for each elementary wave: A_n denotes its complex valued amplitude, ω_n angular frequency and κ_n wave number. We assume that $A_{-n} = A_n^*$, where z^* denotes complex conjugate of z . Since η_l should be a real-valued field, we need to assume that $\omega_{-j} = -\omega_j$ and $\kappa_{-j} = -\kappa_j$. Finally, the linear wave theory postulates that κ and ω are functionally related by the so-called *dispersion relation*

$$\omega^2 = g\kappa \tanh(h\kappa), \quad \omega > 0, \kappa > 0,$$

where g and h are the gravity acceleration and water depth, respectively.

Measurements of the real sea show that the linear wave model is often overly simplistic and leads to errors in the predicted crest height (in deep waters) of about 10-20%. The model can be corrected by using "second-order" terms that allow interactions between the elementary cosine waves. Following Hasselmann (1962), where the detailed derivations are given, the quadratic correction η_q is given by

$$\eta_q(x, t) = \sum_{n=-N}^N \sum_{m=-N}^N \frac{A_n A_m}{2} E(\omega_n, \omega_m) e^{i(\omega_n t - \kappa_n x)} e^{i(\omega_m t - \kappa_m x)}, \quad (5)$$

where the amplitudes A , angular frequencies ω and wave numbers κ satisfy the same relations as in the linear model. The quadratic-transfer function $E(\omega, \tilde{\omega})$, taken from Marthinussen and Winterstein (1992), is given by

$$E(\omega, \tilde{\omega}) = \frac{\frac{g\kappa\tilde{\kappa}}{\omega\tilde{\omega}} - \frac{1}{2g}(\omega^2 + \tilde{\omega}^2 + \omega\tilde{\omega}) + \frac{g}{2} \frac{\omega\tilde{\kappa}^2 + \tilde{\omega}\kappa^2}{\omega\tilde{\omega}(\omega + \tilde{\omega})}}{1 - g \frac{\kappa + \tilde{\kappa}}{(\omega + \tilde{\omega})^2} \tanh(\kappa + \tilde{\kappa})h} - \frac{g\kappa\tilde{\kappa}}{2\omega\tilde{\omega}} + \frac{1}{2g}(\omega^2 + \tilde{\omega}^2 + \omega\tilde{\omega}), \quad (6)$$

where $\kappa, \tilde{\kappa}$ are wave numbers which are computed using the dispersion relation from the angular frequencies $\omega, \tilde{\omega}$, respectively. We also assume that $E(\omega, -\omega) = 0$. It is important to note that for any positive ω and $\tilde{\omega}$ the following symmetry relations hold: $E(\omega, \tilde{\omega}) = E(\tilde{\omega}, \omega)$, $E(\omega, \tilde{\omega}) = E(-\omega, -\tilde{\omega})$ and $E(\omega, -\tilde{\omega}) = E(-\omega, \tilde{\omega})$. These properties imply that η_q is a real-valued field.

The deterministic Second-Order Stokes Wave is thus defined as

$$\eta^N(x, t) = \eta_l(x, t) + \eta_q(x, t), \quad (7)$$

where η_l and η_q are the linear and quadratic processes given by Eqs. 4 and 5, respectively. The Gaussian second-order sea is obtained by assuming that the complex amplitudes A_n , $n > 0$, are independent and normally distributed variables, i.e. $A_n = \sigma_n(U_n - iV_n)$, where U_n, V_n are independent zero mean and variance one Gaussian variables, and σ_n^2 is the energy of waves with angular frequencies ω_n and $-\omega_n$.

Often it is assumed that the linear Gaussian process η_l has a spectral density. For a sea model with linear one-sided spectrum $S(\omega)$, $0 \leq \omega \leq \omega_c$, where ω_c is the cut off frequency, we define $\eta(x, t) = \lim_{N \rightarrow \infty} \eta^N(x, t)$, where $\eta^N(x, t)$ is given by Eq. 7. The individual waves have angular frequencies $\omega_j = j\omega_c/N$ and energy $\sigma_j^2 = S(\omega_j)\Delta\omega$, $j = 1, \dots, N$, while $\Delta\omega = \omega_c/N$.

In the following we use $\eta^N(0, t)$, but in order to simplify the notation we shall write $\eta(t)$ for $\eta^N(0, t)$. In matrix form, if we define

$$\mathbf{Z}(t) = [(U_1 - iV_1)e^{i\omega_1 t} \dots (U_N - iV_N)e^{i\omega_N t}]^T = \mathbf{X}(t) + i\mathbf{Y}(t),$$

and

$$\begin{aligned} \mathbf{Q} &= [q_{mn}], & q_{mn} &= (E(\omega_m, -\omega_n) + E(\omega_m, \omega_n))\sigma_m\sigma_n, \\ \mathbf{R} &= [r_{mn}], & r_{mn} &= (E(\omega_m, -\omega_n) - E(\omega_m, \omega_n))\sigma_m\sigma_n, \\ \boldsymbol{\sigma} &= [\sigma_n], & \sigma_n &= \sqrt{S(\omega_n)\Delta\omega}, \end{aligned} \quad (8)$$

where $m, n = 1, \dots, N$, then

$$\eta(t) = \boldsymbol{\sigma}^T \mathbf{X}(t) + \frac{1}{2} \mathbf{X}(t)^T \mathbf{Q} \mathbf{X}(t) + \frac{1}{2} \mathbf{Y}(t)^T \mathbf{R} \mathbf{Y}(t). \quad (9)$$

MEAN UPCROSSING INTENSITY

Assume that $\eta(t)$ is a stationary, zero mean Gaussian process. If the derivative $\dot{\eta}(t)$ exists then, for a fixed level u , the expected number of times the process $\eta(t)$ crosses u in the upward direction $\mu^+(u)$, is given by

$$\mu^+(u) = \int_0^{+\infty} z f_{\eta(0), \dot{\eta}(0)}(u, z) dz, \quad (10)$$

where $f_{\eta(0), \dot{\eta}(0)}(u, z)$ is the joint density of $\eta(0), \dot{\eta}(0)$. The above classical result is called Rice's formula; see Leadbetter et al. (1983) for a proof. It is easy to check that inserting the Gaussian density of $\eta(0), \dot{\eta}(0)$ into Eq. 10 will give Eq. 2, with $T_z = 2\pi\sqrt{\lambda_0/\lambda_2}$ and $H_s = 4\sqrt{\lambda_0}$, where

$$\lambda_i = \int_0^\infty \lambda^i S(\lambda) d\lambda, \quad (11)$$

since $\text{Var}(\eta(0)) = \lambda_0$ and $\text{Var}(\dot{\eta}(0)) = \lambda_2$.

In the engineering literature, Eq. 10 is often used to compute the upcrossing intensity $\mu^+(u)$ even for non-Gaussian processes as long as the density of $\eta(0), \dot{\eta}(0)$ is available. Since the density is not uniquely defined, Eq. 10 can not be true without some additional conditions. However, if we replace $=$ by $\stackrel{\text{a.a.u.}}{=}$, meaning that the equality is valid for almost all u , Eq. 10 remains true. See Zähl (1984) and Rychlik (2000) for a proof and applications of Rice's formula in oceanography.

By Eq. 10, the computation of $\mu^+(u)$ requires the knowledge of the joint density of $\eta(0), \dot{\eta}(0)$. An explicit closed form formula for the joint density of $\eta(0), \dot{\eta}(0)$, for the process $\eta(t)$ defined by Eq. 9, is not known at present (except when $N = 1$). Here we propose to use saddlepoint methods to approximate $\mu^+(u)$. In order to employ the methods we need the explicit formula for the cumulant generating function of $\eta(0), \dot{\eta}(0)$.

The cumulant generating function, $K(s, t)$, of $\eta(0), \dot{\eta}(0)$ is defined as

$$K(s, t) = \ln(\mathbb{E}[\exp\{s\eta(0) + t\dot{\eta}(0)\}]), \quad (s, t) \in \mathcal{X}, \quad (12)$$

where \mathcal{X} is the set of arguments for which the last integral converges. For the process represented by Eq. 9 we have that (see Machado and Rychlik (2002) for details)

$$K(s, t) = -\frac{1}{2} \ln(\det(\mathbf{I} - \mathbf{A})) + \frac{1}{2} \mathbf{t}^T (\mathbf{I} - \mathbf{A})^{-1} \mathbf{t}, \quad (s, t) \in \mathcal{X}, \quad (13)$$

where the matrix $\mathbf{A} = \mathbf{A}(s, t)$ and the vector $\mathbf{t} = \mathbf{t}(s, t)$ are defined as follows

$$\mathbf{A}(x, y) = \begin{bmatrix} x\mathbf{Q} & y\mathbf{S} \\ y\mathbf{S}^T & x\mathbf{R} \end{bmatrix}, \quad \mathbf{t}(x, y) = \begin{bmatrix} x\boldsymbol{\sigma} \\ y\mathbf{W}\boldsymbol{\sigma} \end{bmatrix}. \quad (14)$$

In the matrices above,

$$\begin{aligned} \mathbf{W} &= [w_{mn}], \quad w_{mm} = -\omega_m, \quad \text{and } w_{mn} = 0 \text{ if } m \neq n, \\ \mathbf{S} &= \mathbf{Q}\mathbf{W} - \mathbf{W}\mathbf{R}, \end{aligned} \quad (15)$$

where $m, n = 1, \dots, N$, and $\mathbf{Q}, \mathbf{R}, \boldsymbol{\sigma}$ are given by Eq. 8.

SADDLEPOINT METHODS

The saddlepoint approximation was first introduced by Daniels (1954, 1987) as a formula to approximate the probability density function from its cumulant generating function. We shall apply here a variant of the method which will allow us to obtain directly an approximation of $\mu^+(u)$.

We start by writing Eq. 10 as a function of $K(s, t)$, and eliminate the integration on z

$$\mu^+(u) = \lim_{y \rightarrow 0} \frac{1}{(2\pi i)^2} \int_{\hat{t}-i\infty}^{\hat{t}+i\infty} \int_{-i\infty}^{+i\infty} \frac{1}{t^2} e^{K(s,t) - su - ty} ds dt. \quad (16)$$

(The limit $y \rightarrow 0$ is introduced for some technical reasons.) In addition, the path of integration in dt has been deformed to the vertical line with $Re(t) = \hat{t} > 0$ to avoid the singularity at $t = 0$. Then the inner integral in ds is approximated

by means of the one-dimensional saddlepoint approximation, also sometimes called *Laplace method*,

$$\frac{1}{2\pi i} \int_{-i\infty}^{+i\infty} e^{K(s,t) - su - ty} ds \approx \frac{1}{\sqrt{2\pi}} h(t) e^{g(t)}, \quad (17)$$

where, if we denote $L(s, t) = K(s, t) - su - ty$,

$$g(t) = L(s_t, t), \quad h(t) = (L''(s_t, t))^{-\frac{1}{2}}, \quad (18)$$

and s_t is the local minimum of $L(s, t)$, for fixed t values.

Now, using Eq. 17 the upcrossing intensity can be approximated as

$$\mu^+(u) \approx \lim_{y \rightarrow 0} \frac{1}{\sqrt{2\pi}} \frac{1}{(2\pi i)} \int_{\hat{t}-i\infty}^{\hat{t}+i\infty} \frac{h(t)}{t^2} e^{g(t)} dt. \quad (19)$$

The double pole of the integrand in Eq. 19 at $t=0$ makes the computation of any approximation for the integral somewhat difficult. However there are special cases when the integral can be computed "almost" explicitly; see the following example.

Example: Suppose that the functions $g(t)$ and $h(t)$, in Eq. 19, are quadratic polynomials, e.g.

$$g(t) = \frac{at^2}{2} + bt + c, \quad h(t) = \frac{At^2}{2} + Bt + C,$$

where $a > 0$. Assume that we can choose \hat{t} to be the position of the local minimum of $\frac{at^2}{2} + bt + c$. Then the integral in Eq. 19 can be evaluated as follows

$$\begin{aligned} & \frac{1}{(2\pi i)} \int_{\hat{t}-i\infty}^{\hat{t}+i\infty} \frac{h(t)}{t^2} e^{g(t)} dt = \\ & e^c \left(\frac{A}{2\sqrt{a}} \phi(\sqrt{a}\hat{t}) + B\bar{\Phi}(\sqrt{a}\hat{t}) + \sqrt{a}C\Psi(\sqrt{a}\hat{t}) \right), \end{aligned} \quad (20)$$

where $\phi(x)$ is the standard Gaussian density, $\bar{\Phi}(x) = \int_x^\infty \phi(y) dy$ and $\Psi(x) = \int_x^\infty \bar{\Phi}(y) dy$. Note that both $\bar{\Phi}$ and Ψ functions can not be computed analytically, however very accurate approximations do exist. These functions are included in most numerical toolboxes. For the sea model we will need only the values of the functions for $x = 0$. For this special case we know that $\bar{\Phi}(0) = 1/2$ while $\phi(0) = \Psi(0) = 1/\sqrt{2\pi}$.

Proceeding in a similar way as in the last example we can approximate $g(t)$ and $h(t)$ by suitable polynomials (the symmetry $K(s, t) = K(s, -t)$ is also employed; see Butler et al. (2002) for more details). Next letting y go to zero we derive the following approximation for the upcrossing intensity

$$\mu^+(u) \approx \hat{f}(u) \frac{\sqrt{g''(0)}}{\sqrt{2\pi}} \left(1 + \frac{h''(0)}{2h(0)g''(0)} - \frac{1}{24} \frac{g^{iv}(0)}{g''(0)^2} \right), \quad (21)$$

where $g(t) = K(s_t, t) - s_t u$, $h(t) = \frac{1}{\sqrt{K_{11}(s_t, t)}}$ and s_t satisfies $K_1(s_t, t) = u$. Here

$$K_1(s, t) = \frac{\partial K(s, t)}{\partial s}, \quad K_{11}(s, t) = \frac{\partial^2 K(s, t)}{\partial s^2},$$

and $\hat{f}(u)$ is the saddlepoint approximation for the density of $\eta(0)$ given by

$$\hat{f}(u) = \frac{h(0)}{\sqrt{2\pi}} e^{g(0)}. \quad (22)$$

It is well known that the saddlepoint density often does not integrate to one, i.e. it is not necessarily a probability density function (*pdf*). Accuracy can often be improved (see Durbin, 1980) by scaling $\hat{f}(u)$ so that it integrates to 1. We denote this scaled saddlepoint approximation as $\bar{f}(u)$ and we shall use it in our examples, i.e. we define our final saddlepoint approximation $\bar{\mu}^+(u)$ as follows:

$$\bar{\mu}^+(u) = \bar{f}(u) \frac{\sqrt{g''(0)}}{\sqrt{2\pi}} \left(1 + \frac{h''(0)}{2h(0)g''(0)} - \frac{1}{24} \frac{g^{iv}(0)}{g''(0)^2} \right) \approx \mu^+(u). \quad (23)$$

Numerical remarks: In order to evaluate Eq. 23 we need to first find the value s_0 , which is an implicitly defined function of the level u , i.e. $K_1(s_0, 0) = u$. By knowing the value $s = s_0(u)$ the cumulative generating function $K(s, 0)$ and its derivatives $K_1(s, 0)$, $K_{11}(s, 0)$, the function $\hat{f}(s)$ can be computed, since

$$g(0) = K(s, 0) - sK_1(s, 0), \quad h(0) = \frac{1}{\sqrt{K_{11}(s, 0)}}, \\ g''(0) = K_{22}(s, 0), \quad (24)$$

where $K_{22}(s, t) = \frac{\partial^2 K(s, t)}{\partial t^2}$. Next we compute the integral $I = \int \hat{f}(u) du$ and define the normalized saddlepoint density $\bar{f}(u) = \hat{f}(u)/I$.

Longer but still elementary derivations are needed to derive the term in Eq. 23 as

$$\frac{h''(0)}{2h(0)g''(0)} = -\frac{1}{4} \frac{K_{1122}(s, 0)K_{11}(s, 0) - K_{111}(s, 0)K_{122}(s, 0)}{K_{11}(s, 0)^2 K_{22}(s, 0)}, \\ \frac{g^{iv}(0)}{g''(0)^2} = \frac{K_{2222}(s, 0)K_{11}(s, 0) - 3K_{122}(s, 0)^2}{K_{11}(s, 0)K_{22}(s, 0)^2}. \quad (25)$$

Here $K_{1122}(s, t)$ means that the cumulant generating function $K(s, t)$ is twice differentiated on s and twice on t while $K_{122}(s, t)$ indicates differentiation once on s and twice on t . The other derivatives are defined in a similar way. Since for the second-order random sea the cumulant generating function, given by Eq. 13, is a complicated expression, the partial derivatives of $K(s, t)$ have to be computed numerically.

¹The spectrum is a parametric formula that was derived in the JOint North Sea WAve Project carried out, during 1968 and 1969, in the North Sea; Hasselmann et al. 1973.

²The spectrum is based on a similarity law, and its validity is verified through the analysis of 3 data sets from: TEXEL, MARSEN projects (North Sea) and ARSLOE project (Duck, North Carolina, USA); Bouws et al. 1985.

Next we comment on the issue of finding $s = s_0$, i.e. solving $K_1(s_0, 0) = u$. In order to avoid solving this non-linear equation we propose here to use the inverse function $s \rightarrow u = K_1(s, 0)$, which is easy to evaluate. More precisely we choose a vector of s values and compute the corresponding $u(s)$ levels and the constants defined by Eqs. 24-25, so that the approximation of the upcrossing intensity $\bar{\mu}^+(u(s))$ can be evaluated by means of Eq. 23. If we wish to know the upcrossing intensity for a particular u value, we use splines to extend $\bar{\mu}^+(u(s))$ to $\bar{\mu}^+(u)$.

Finally, since Eqs. 25 involve higher-order partial derivatives of $K(s, t)$, we have also checked an alternative approach, which is to compute numerically $g''(0)$, $g^{iv}(0)$ and $h''(0)$ from $g(t)$, $h(t)$, respectively. This approach is more complicated than the computations of the K derivatives, and hence slower. Since it did not give more accurate values and also was more unstable for low u -values, we have not incorporated it into our programs. The programs are included in WAFO (Wave Analysis for Fatigue and Oceanography)-toolbox, available free of charge at <http://www.maths.lth.se/matstat/wafo/>; see Brodtkorb et al. (2000).

NUMERICAL EXAMPLES

In this section we shall demonstrate the accuracy of the saddlepoint approximation for the crossing intensity, by presenting the relative errors of estimation for three examples.

The first example considers the Narrow-band Stoke's waves in deep waters, when the transfer function $E(\omega, \tilde{\omega})$ is particularly simple, viz.

$$E(\omega_m, -\omega_n) = 0, \quad E(\omega_m, \omega_n) = \frac{\omega_p^2}{2g}, \quad n, m = 1, \dots, N,$$

where ω_p is the peak frequency of the spectrum $S(\omega)$ of the linear part $\eta_l(t)$. We select $S(\omega)$ to be a JONSWAP¹ spectrum, which is a parametric (analytical) formula. The parameters chosen here are significant wave height $H_s = 7$ [m], peak period $T_p = 11$ [sec] and peak-shape parameter $\gamma = 2.385$. The chosen cut off frequency is $\omega_c = 3$ [rad/sec], i.e. $S(\omega) = 0$ for $\omega > \omega_c$. The peak frequency is then $\omega_p = 0.574$ [rad/sec].

In the second example, we shall still consider a deep water location with the same JONSWAP spectrum for the linear part, but the transfer function $E(\omega, \tilde{\omega})$ will be given by Eq. 6. Since $h = \infty$ then $E(\omega, \tilde{\omega})$ simplifies to

$$E(\omega, \tilde{\omega}) = \begin{cases} -\frac{1}{2g} |\omega^2 - \tilde{\omega}^2| & \text{if } \omega\tilde{\omega} < 0, \\ \frac{1}{2g} (\omega^2 + \tilde{\omega}^2) & \text{otherwise.} \end{cases}$$

Finally in the last example the water depth is chosen to be finite and hence $E(\omega, \tilde{\omega})$, given by Eq. 6, will be more complicated. In order to connect to the previous examples we shall now use the so-called TMA² spectrum. This is the

expected spectrum in finite water depths, created by the meteorological conditions which caused the JONSWAP spectrum at deep waters. (Obviously both JONSWAP and TMA spectra are only models for the true-unknown sea spectra.)

It will be shown on the second and third examples, that for positive u levels, the saddlepoint approximation $\bar{\mu}^+(u)$ is very accurate with relative errors of a few percent. For the narrow-band Stoke's sea the relative error is below 10 % which is an acceptable accuracy. Next the function $\bar{\mu}^+(u)$ will be used to evaluate the bound defined in Eq. 1 for the distribution of wave crest height. The accuracy of the bound will be checked by means of simulations.

Since the approximation of crest distribution based on $\mu^+(u)$ is more accurate for higher waves, we exclude the small waves, and compare the approximation of the conditional distribution of the crest height given that it is higher than $h_0 = 1$ meter, viz.

$$P(A_c > h | A_c > h_0) \approx \frac{\bar{\mu}^+(h)}{\bar{\mu}^+(h_0)}, \quad (26)$$

with simulations. More precisely, since the exact distribution of crest height is not known at present we shall compare the proposed approximation with the empirical conditional distribution obtained from the simulated process $\eta(t)$, $0 \leq t \leq T$, sampling frequency 5 [Hz] and $T = 24$ [hours]. Although it is seldom that the sea surface elevation can be described by the same model for longer periods than a few hours, we have chosen such a long T in order to reduce the variance of the estimate.

In all three examples the approximation defined by Eq. 26 is very accurate. These particularly good results can be explained by the fact that the relative error of the saddlepoint approximation $\bar{\mu}^+(u)$ is almost constant for positive u values and hence the errors cancel, i.e. $\frac{\bar{\mu}^+(h)}{\bar{\mu}^+(h_0)}$ is close to $\frac{\mu^+(h)}{\mu^+(h_0)}$.

Example 1: Narrow-band Stoke's waves

Let us consider the sea containing only one Gaussian cosine wave, i.e. $\eta(t) = \sigma R \cos(\omega t + \phi)$, where R is a standard Rayleigh distributed variable and ϕ is a uniformly distributed random phase, which is independent of R . As before σ^2 is the energy of the wave. The Hilbert transform of the cosine wave is $\eta_H(t) = \sigma R \sin(\omega t + \phi)$. The Stoke's wave can then be written as follows:

$$\begin{aligned} \eta(t) &= \sigma R \cos(\omega t + \phi) + \frac{\omega^2}{2g} \sigma^2 R^2 \cos(2\omega t + 2\phi) \quad (27) \\ &= \eta(t) + \frac{1}{2\kappa} (\eta(t)^2 - \eta_H(t)^2), \end{aligned}$$

where $\kappa = g/\omega^2$ is the wave number (in deep waters) of the wave with frequency ω . We shall now generalize Eq. 27 and let $\eta(t)$ be a Gaussian sea with spectrum $S(\omega)$ while $\eta_H(t)$ be its Hilbert transform. (It is well known that $\eta_H(t)$ is also a Gaussian process defined by adding $-\pi/2$ to the phases of all individual cosine waves constituting η ; see Cramér and

Leadbetter (1967) for discussion of the properties of $\eta_H(t)$.) Next let

$$\eta(t) = \eta(t) + \frac{1}{2\kappa_p} (\eta(t)^2 - \eta_H(t)^2), \quad (28)$$

where $\kappa_p = g/\omega_p^2$ and ω_p is the peak frequency of the spectrum $S(\omega)$. (The $S(\omega)$ chosen in the numerical computations gives $\kappa_p = 29.76$ [rad/m].)

In oceanography the process (Eq. 28) is sometimes used to model sea surface elevation when the power spectrum is concentrated around the peak frequency ω_p and therefore all waves have its wave numbers close to κ_p . Such sea is called *narrow-band*. The crest distribution for the process Eq. 28 is unknown, however some approximations do exist; see Prevosto et al. (2000).

In order to compute the saddlepoint approximation of the crossing intensity, we need the cumulant generating function $K(s, t)$. Since the process $\eta(t)$, defined by Eq. 28, can also be written using Eq. 9 we can use Eq. 13 to compute $K(s, t)$. However, the evaluation of Eq. 13 involves finding eigenvalues and eigenvectors of the matrix: $\mathbf{I} - \mathbf{A}$, which is at least a (500,500)-matrix; see Langley (1987) for details. Since for the process (Eq. 9) an explicit simple formula for $K(s, t)$ exists, see Eq. 30, we shall use it instead. (Observe that in Examples 2,3 there are no simpler formulas to be used.)

The possibility of computing $K(s, t)$ by two alternative ways is one of the reasons why we are more extensively studying the narrow band case. Namely we can check the numerical stability of the computation of the derivatives of $K(s, t)$ defined by Eq. 13. We discovered that the computed approximations $\bar{\mu}^+(u)$ using the cumulant generating functions defined by Eq. 13 and Eq. 30 are almost identical. The relative errors differs by 0.05 % and hence can be disregarded. We expect that the error is of the same order for the general process (Eq. 9), in Examples 2,3, where no simpler expression for the cumulant generating function is available.

Cumulant generating function for $\eta(t)$ in Eq. 28: Consider the following vector $[\eta(0) \eta_H(0) \dot{\eta}(0) \dot{\eta}_H(0)]^T$ of zero mean Gaussian variables, with covariance matrix

$$\Sigma = \begin{bmatrix} \lambda_0 & 0 & 0 & \lambda_1 \\ 0 & \lambda_0 & -\lambda_1 & 0 \\ 0 & -\lambda_1 & \lambda_2 & 0 \\ \lambda_1 & 0 & 0 & \lambda_2 \end{bmatrix}, \quad (29)$$

in which λ_i are the spectral moments defined by Eq. 11. In this case, we can compute $K(s, t)$ by employing its definition, Eq. 12, together with some mathematical manipulation:

$$K(s, t) = -\log(\lambda_0) - \frac{1}{2} \log(\det(\mathbf{A})) + \frac{\sigma^2}{2} t^2 + \frac{\kappa_p^2}{2} \mathbf{t}^T \mathbf{A}^{-1} \mathbf{t}, \quad (30)$$

where $\sigma^2 = \left(\lambda_2 - \frac{\lambda_1^2}{\lambda_0} \right)$, and the (2,2)-matrix $\mathbf{A} = \mathbf{A}(s, t)$

and the vector $\mathbf{t} = \mathbf{t}(s, t)$ are defined as follows

$$\mathbf{A}(s, t) = \begin{bmatrix} -\frac{s}{\kappa_p} - \sigma^2 \left(\frac{t}{\kappa_p}\right)^2 + \frac{1}{\lambda_0} & 2\frac{\lambda_1}{\lambda_0} \frac{t}{\kappa_p} \\ 2\frac{\lambda_1}{\lambda_0} \frac{t}{\kappa_p} & \frac{s}{\kappa_p} - \sigma^2 \left(\frac{t}{\kappa_p}\right)^2 + \frac{1}{\lambda_0} \end{bmatrix}$$

and

$$\mathbf{t}(s, t)^T = \begin{bmatrix} \frac{s}{\kappa_p} + \sigma^2 \left(\frac{t}{\kappa_p}\right)^2 & -\frac{\lambda_1}{\lambda_0} \frac{t}{\kappa_p} \end{bmatrix}.$$

The matrix \mathbf{A} in Eq. 30 is only $(2, 2)$, thus its determinant and inverse are easy to write in an explicit analytical way. Note that the $K(s, 0)$ function is defined for $s \in (-\kappa_p/\lambda_0, \kappa_p/\lambda_0)$.

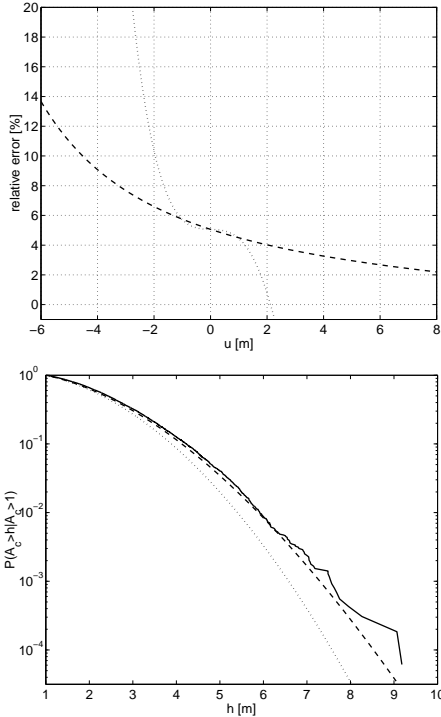


FIG. 1 The saddlepoint approximation applied for narrow-band Stoke's sea. *Top* Relative errors of the approximations $\bar{\mu}^+(u)$ (dashed line) and Eq. 2 (dotted line). *Bottom* Conditional distribution of crest amplitudes A_c , i.e. $P(A_c > h | A_c > 1)$, h [m]. Irregular line: empirical distribution estimated from simulated 24-hour-long narrow-band Stoke's sea, dotted line: Gaussian approximation ($\eta = \eta_l$), i.e. the distribution of A_c given in Eq. 3 and dashed line: the approximation based on $\bar{\mu}^+(u)$, using Eq. 26.

We turn now to evaluation of accuracy of saddlepoint approximation of crossing intensity $\mu^+(u)$. In all figures, lines that represent results derived from the “exact” crossing intensity $\mu^+(u)$ will be presented by (solid lines), using $\bar{\mu}^+(u)$ by (dashed lines), while the (dotted line) will be used to represent results for linear Gaussian sea, i.e. $\eta = \eta_l$. The accuracy of the saddlepoint approximation, with generic notation f^{spm} , will be measured by means of the relative error

defined as

$$E_{rel}(u) = (f^{spm}(u) - f^{exact}(u)) / f^{exact}(u) \cdot 100 [\%],$$

where $f^{exact}(u)$ is the target value to approximate.

First we check the accuracy of the normalized saddlepoint approximation of the density of $\eta(0)$, $\bar{f}(u)$. Since $\hat{f}(u)$ integrates to 1.0013, $\bar{f}(u) \approx \hat{f}(u)$, however we still need to check how close $\bar{f}(u)$ is to the true density $f_{\eta(0)}$. The true density is not given by an explicit formula and has to be computed numerically using the one-dimensional integration; see Eq. 31. The accuracy of $\bar{f}(u)$ is remarkable with the relative error around 0.1% for $u \in [-6, 9]$. (Note that in Examples 2,3 there is no formula for the density of $\eta(0)$ available.)

Next, we check the approximation $\bar{\mu}^+(u)$ of the crossing intensity $\mu^+(u)$. The relative error is presented in Fig. 1 (*Top*). The crossing intensity $\mu^+(u)$ is computed by using Eq. 32, while saddlepoint approximation $\bar{\mu}^+(u)$ by means of Eq. 23, with $K(s, t)$ given in Eq. 30. The approximation $\bar{\mu}^+(u)$ is performing very well giving a relative error below 10% as can be seen in Fig. 1 (*Top*).

Finally we turn to the main subject of the paper, the approximation of the distribution of crest height defined by Eq. 1. As shown in Fig. 1 (*Bottom*), the accuracy of the proposed approximation is very good. We can also see that the Rayleigh distribution, defined by the right hand side of Eq. 3 with $H_s = 7$ [m], clearly underestimates the wave heights.

Example 2: JONSWAP spectrum (deep waters)

As in the previous example we begin with computation of the saddlepoint approximation $\hat{f}(u)$. Here the integral $I = \int \hat{f}(u) du = 0.9997$. This means that the approximation is almost a pdf. However, the true density of $\eta(0)$ is not known for the process and hence we can not compare $\bar{f}(u)$ with $f_{\eta(0)}(u)$. We turn directly to the analysis of the accuracy of the approximation $\bar{\mu}^+(u)$, defined by Eq. 23 with $K(s, t)$ given by Eq. 13, of the mean upcrossing intensity $\mu^+(u)$. Here we have an additional difficulty in that we do not have any simple method to evaluate $\mu^+(u)$. Therefore, we consider the $\mu^+(u)$ values computed with the numerical methods used by Næss and Machado (2000) as the target values for the approximation. We shall refer to this method here by numerical method. The relative error is presented in Fig. 2 (*Top*) and we can see that the relative error is much smaller in this example. Finally, in Fig. 2 (*Bottom*) the accuracy of the approximation of the conditional distribution of the crest height given that crests are higher than one meter is presented. In the figure we can see excellent agreement between the approximation and the empirical distribution obtained from simulated sea surface elevation.

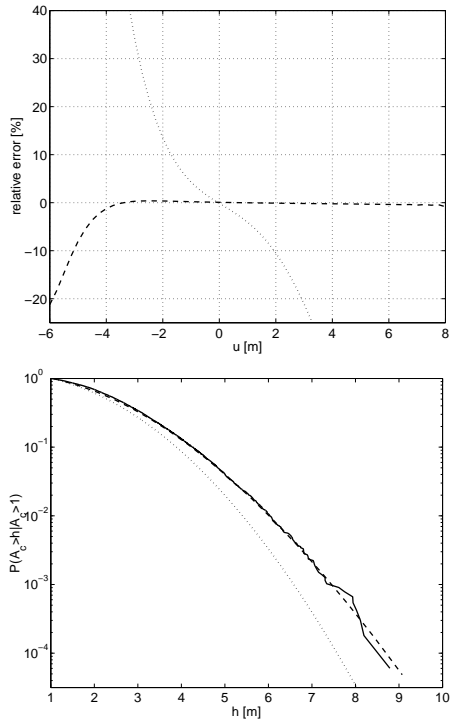


FIG. 2 The saddlepoint approximation applied for second order model for sea at infinite depth and JONSWAP spectrum. *Top* Relative errors of the approximations $\bar{\mu}^+(u)$ (dashed line) and Eq. 2 (dotted line). *Bottom* Conditional distribution of crest amplitudes A_c , i.e. $P(A_c > h | A_c > 1)$, h [m]. Irregular line: empirical distribution estimated from simulated 24-hour-sea elevation, dotted line: Gaussian approximation ($\eta = \eta_l$), i.e. the distribution of A_c given in Eq. 3 and dashed line: the approximation based on $\bar{\mu}^+(u)$, using Eq. 26.

Note that the distribution of the crest height for the narrow band Stoke's sea and the complete quadratic-model differ marginally from each other. We shall quantify this by giving the size of the so-called *10 days crest height*, i.e. if the sea had the same JONSWAP spectrum for 10 days, than (on average) one wave in 10 days would have crest higher than the *10 days crest*. The 10 days crest height is predicted to be 8.4 [m], 9.6 [m] and 9.8 [m], if we model the surface by means of a Gaussian linear sea η_l , the narrow-band Stokes sea (defined by Eq. 28) and the second-order sea (defined by Eq. 9), respectively.

Example 3: TMA spectrum (finite depth)

In this final example we consider the sea surface elevation in finite water depth conditions. The sea is modeled by means of the second-order random sea defined by Eq. 9 with a transfer function E given by Eq. 6 with a water depth of $h = 20$ [m]. Here we shall use the TMA-spectrum which is the transform of the JONSWAP spectrum from Examples 1,2 to the finite depth location. Here the waves will be smaller but the asymmetry between crests and troughs

is more transparent. This can be seen in the plot of $\bar{\mu}^+(u)$ given in Fig. 3 (*Top*). Here we shall not show the plot of the relative error, but it is similar to the one given in the previous example. (The relative error of the saddlepoint approximation is small (below 2 %) for positive u values.) In Fig. 3 (*Bottom*) the accuracy of the approximation of the conditional distribution of the crest height given that crests are higher than one meter is presented. As before we can see the excellent agreement between the approximation and the empirical distribution estimated from simulated sea surface elevation.

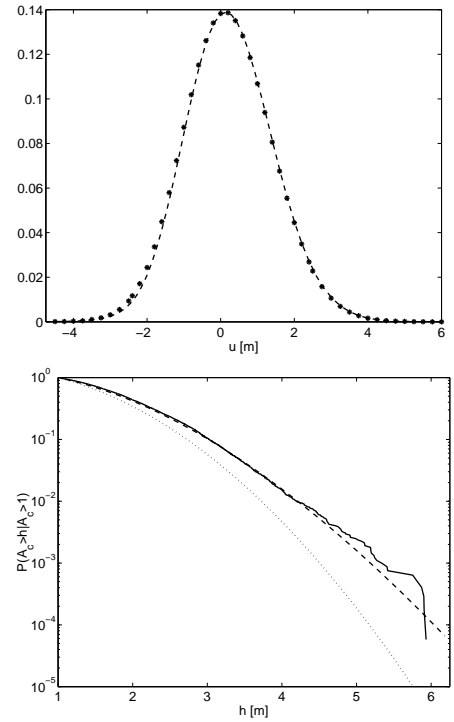


FIG. 3 The saddlepoint approximation applied for second-order model for sea at 20 meters depth and TMA spectrum. *Top* Comparison of $\bar{\mu}^+(u)$ (dashed line) and the $\mu^+(u)$ computed using the numerical method (stars). *Bottom* Conditional distribution of crest amplitudes A_c , i.e. $P(A_c > h | A_c > 1)$, h [m]. Irregular line: empirical distribution estimated from simulated-24-hours sea elevation, dotted line: Gaussian approximation ($\eta = \eta_l$), i.e. the distribution of A_c given in Eq. 3 and dashed line: the approximation based on $\bar{\mu}^+(u)$, using Eq. 26.

CONCLUSIONS

In the paper we have demonstrated that the crest distribution of the waves in the second-order random sea model, defined by Eq. 9, can be very accurately approximated by Eq. 26. The formulas for the crossing intensity are explicit but contain higher-order derivatives of the cumulant generating function, which usually have to be computed numerically. The programs in MATLAB computing the saddlepoint approximation of the crossing intensity are avail-

able. The proposed method gives results as accurate as the complicated and slow numerical method used by Næss and Machado (2000), with a time reduction from a day to a few seconds. The new method is fast, fully automated and numerically stable. These are important properties if one wishes to compute the distribution of crest height over long periods of time where the sea state varies, i.e. to mixed the distributions presented in the paper.

REFERENCES

- Bouws, E., Gunther, W., Rosenthal, W. and Vincent, C.L. (1985). "Similarity of the wind wave spectrum in finite depth water 1. spectral form," *Journal of Geophysical Research*, Vol 90, pp 975–986.
- Brodtkorb, P. A., Johannesson, P., Lingren, G., Rychlik, I., Rydén, J. and Sjö, E. (2000). "WAFO - a Matlab toolbox for analysis of random waves and loads," *Proc 10th Int Offshore and Polar Eng Conf*, ISOPE, Vol 3, pp 343–350.
- Butler, R., Machado, U.B., and Rychlik, I. (2003). "Saddlepoint approximation of crossing intensities," in preparation.
- Cramér, H. and Leadbetter, M. R. (1967). *Stationary and Related Stochastic Processes*. New York: Wiley.
- Daniels, H. E. (1954). "Saddlepoint approximations in statistics," *Ann Math Statist*, Vol 25, pp 631–50.
- Daniels, H. E. (1987). "Tail probability approximations," *Int. Statist. Rev.*, Vol 55, pp 37-48.
- Durbin, J. (1980). "Approximations for densities of sufficient statistics," *Biometrika*, Vol 67, pp 311-333.
- Hasselmann, K. (1962). "On the non-linear energy transfer in a gravity-wave spectrum, Part 1, General Theory," *J Fluid Mech*, Vol 12, pp 481–500.
- Hasselmann, K., Barnett, T.P., Bouws, E., Carlson, H., Cartwright, D.E., Enke, K., Ewing, J.A., Gienapp, H., Hasselmann, D.E., Kruseman, P., Meerburg, A., Müller, P., Olbers, D.J., Richter, K., Sell, W., and Walden, H. (1973). "Measurements of Wind Wave Growth and Swell Decay During the Joint North Sea Wave Project (JONSWAP)," *Deutsches Hydro. Zeit.*, Reich A12, pp 1–95.
- Langley, R.S. (1987). "A statistical analysis of non-linear random waves," *Ocean Eng*, Vol 14, No 5, pp 389–407.
- Leadbetter, M.R., Lindgren, G. and Rootzén, H. (1983). *Extremes and Related Properties of Random Sequences and Processes*, Springer-Verlag.
- Machado, U.B. and Rychlik, I. (2002). "Wave statistics in nonlinear random sea," to appear in, *Extremes*.
- Marthinsen, T. and Winterstein, S.T. (1992). "On the skewness of random surface waves," *Proceedings of the 2nd International Offshore and Polar Engineering Conference*, ISOPE, Vol III, pp 472–478.
- Næss, A. and Machado, U.B. (2000). "Response statistics of large compliant offshore structures," *Proceedings of the 8th ASCE Specialty Conference on Probabilistic Mechanics and Structure Reliability*, New York.
- Prevosto, M., Krogstad, H.E. and Robin, A. (2000). "Probability distributions for maximum wave and crest heights," *Coastal Engineering*, Vol 40, pp 329–360.
- Rice, S.O. (1944). "The mathematical analysis of random

noise," *Bell Syst. Techn. J.*, Vol 23, pp 282–332.

Rice, S.O. (1945). "The mathematical analysis of random noise, II," *Bell Syst. Techn. J.*, Vol 24, pp 46–156.

Rychlik, I. (1993). "On the "narrow-band" approximation for expected fatigue damage," *Probabilistic Engineering Mechanics*, Vol 8, pp 1–4.

Rychlik, I. (2000). "On some reliability applications of Rice formula for intensity of level crossings," *Extremes*, Vol 3, No 4, pp 331-348.

Rychlik, I. and Leadbetter, M.R. (2000). "Analysis of ocean waves by crossing and oscillation intensities," *International Journal of Offshore and Polar Engineering*, Vol 10, pp 282–289.

Zähle, U. (1984). "A general Rice formula, Palm measures, and horizontal-window conditioning for random fields," *Stochastic Process. Appl.*, Vol 17, pp 265–283.

APPENDIX

Define

$$f(y, z) = \begin{cases} \frac{1}{2\pi} \frac{\kappa_p^2}{\lambda_0 \sqrt{\Delta}} e^{-\frac{\kappa_p^2}{\lambda_0}(1+z+y^2)} \left(e^{\frac{\kappa_p^2}{\lambda_0} \sqrt{\Delta}} + e^{-\frac{\kappa_p^2}{\lambda_0} \sqrt{\Delta}} \right), & \text{if } \Delta(y, z) \geq 0, \\ 0, & \text{otherwise,} \end{cases}$$

where

$$\Delta(y, z) = 1 + 2z + y^2, \text{ where } z \geq -(1 + y^2),$$

then the density of $\eta(0)$ is given by

$$f_{\eta(0)}(z) = \int \frac{1}{\kappa_p} f_{Y,Z} \left(y, \frac{z}{\kappa_p} \right) dy. \quad (31)$$

We turn now to the computation of the crossing intensity $\mu^+(u)$ of the process $\eta(t)$. Let us introduce

$$m(x, y) = -y \frac{\lambda_1}{\lambda_0} (1 + 2x), \quad \sigma(x, y) = \frac{\sigma}{\kappa_p} \sqrt{(y-1)^2 + x^2},$$

then

$$\mu^+(u) = \int_{\Delta(y, u/\kappa_p) \geq 0} \frac{1}{2\pi} \frac{\kappa_p^2}{\lambda_0} \frac{g_1(y, u/\kappa_p) + g_2(y, u/\kappa_p)}{\sqrt{\Delta(y, u/\kappa_p)}} e^{-\frac{\kappa_p^2}{\lambda_0}(1+u/\kappa_p+y^2)} dy, \quad (32)$$

where

$$g_1(y, z) = \sigma(x, y) e^{\frac{\kappa_p^2}{\lambda_0} \sqrt{\Delta(y, z)}} \Psi \left(-\frac{m(x, y)}{\sigma(x, y)} \right), \\ x = -1 + \sqrt{\Delta(y, z)},$$

$$g_2(y, z) = \sigma(x, y) e^{-\frac{\kappa_p^2}{\lambda_0} \sqrt{\Delta(y, z)}} \Psi \left(-\frac{m(x, y)}{\sigma(x, y)} \right), \\ x = -1 - \sqrt{\Delta(y, z)},$$

and $\Psi(x)$ -function is defined by Eq. 20.